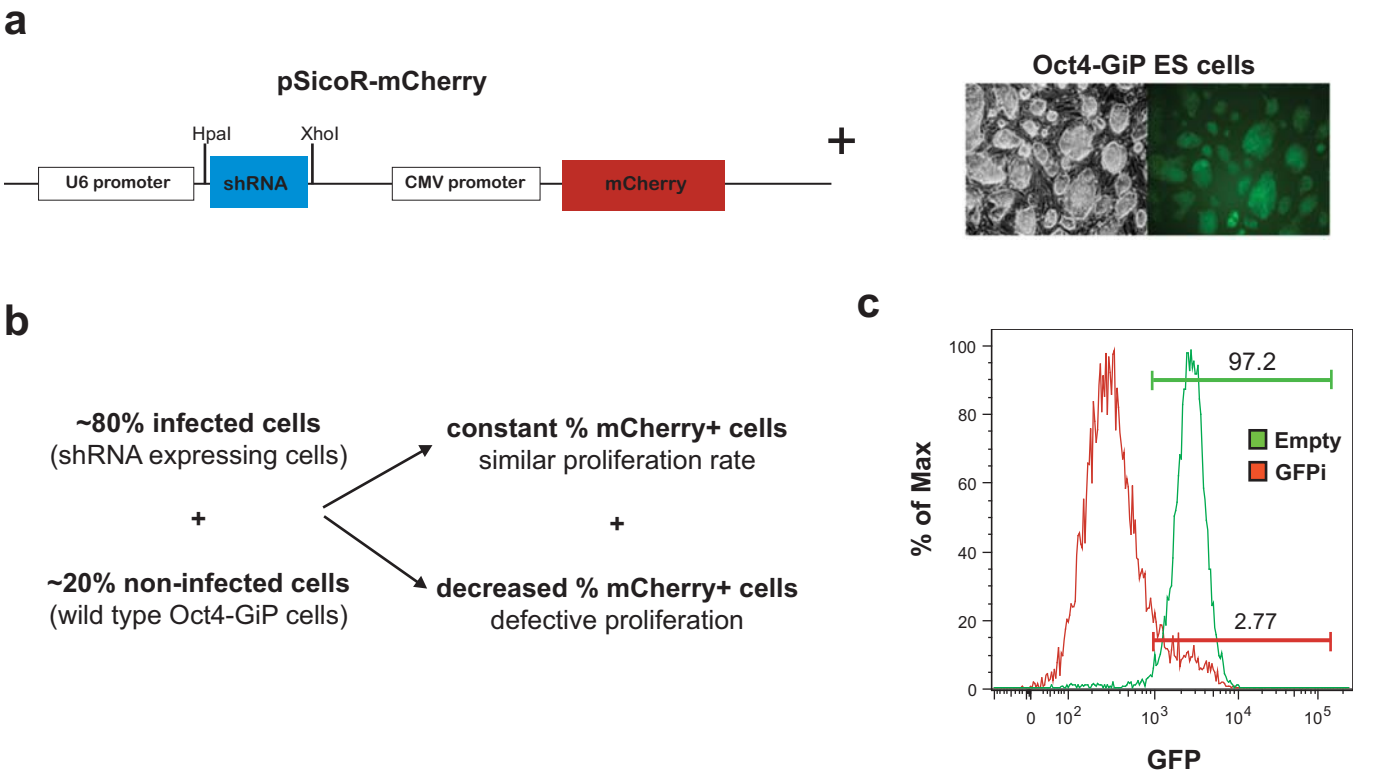

Supplementary Figure 1

Supplementary Figure 1. RNAi screen in mouse ES cells. a, A loss-of-function screen for 41 candidate genes in ES cells. The lentiviral vector pSicoR-mCherry used transcribes a shRNA (under the control of human *U6* promoter) and a reporter red fluorescent protein, mCherry; the ES cell line used expresses GFP under the control of the *Oct4* promoter (*Oct4*-GFP). **b,** A competition assay was performed between infected cells (mCherry+, undergoing RNAi for the gene of interest) and non-infected cells. The proportion of mCherry+ cells was measured by FACS analysis for 5 passages. **c,** FACS plot showing the percentage of GFP+ cells in Oct4-GiP ES cells infected with either the empty vector or with shRNA against GFP. **d,** Knockdown of the three major transcription factors known to regulate ES cells (*Oct4, Sox2* and *Nanog*) leads to decreased proliferation. The proliferation index was measured by comparing the percentage of infected cells in each passage with cells infected with a control virus. Down-regulation of GFP did not affect proliferation of ES cells. The values are represented as mean ± s.d. (n=3) **e,** Summary of the RNAi screen highlighting *Chd1* as a novel regulator of ES cells. 7 genes showed both loss of *Oct4*-GFP activity and proliferation defects (*Chd1, FoxD3, Nanog, Oct4, Sall4, Sox2, Utf1*). 6 of the genes that showed proliferation defects had not previously been implicated in ES cells (*Chd1, Cbf, Ddx18, NFYa, NFYb, Terf1*), and were confirmed by two independent shRNAs. A detailed description of the RNAi phenotype of *NFYa* and *NFYb* have recently been described[7].

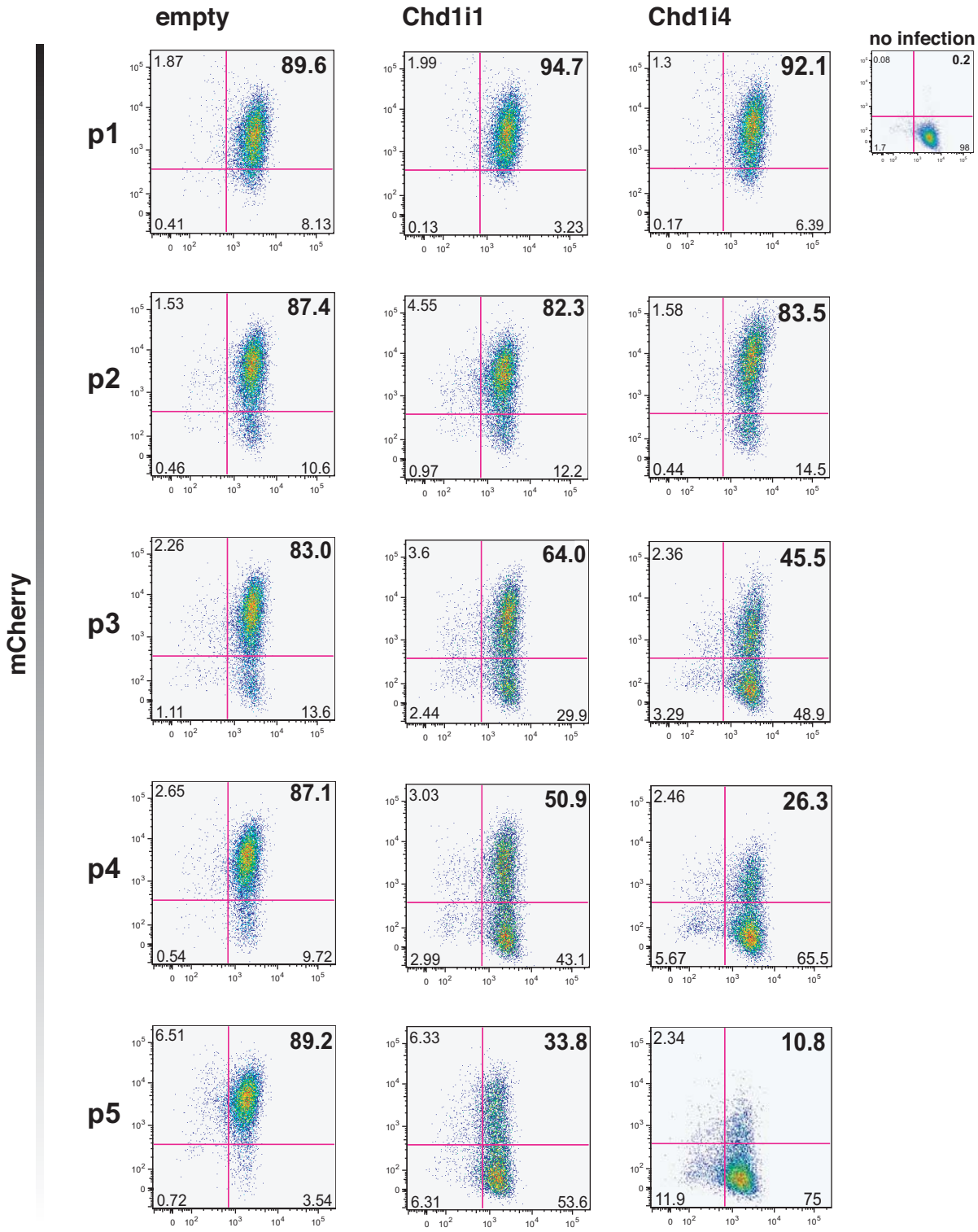

Supplementary Figure 2

Supplementary Figure 2. *Chd1* RNAi in mouse ES cells. FACS plots showing mCherry and GFP fluorescence of Oct4-GiP ES cells infected with pSicoR-mCherry with shRNAs against *Chd1* or empty vector, over 5 passages. Highlighted on the top right side of each plot is the percentage of mCherry+/GFP+ cells.

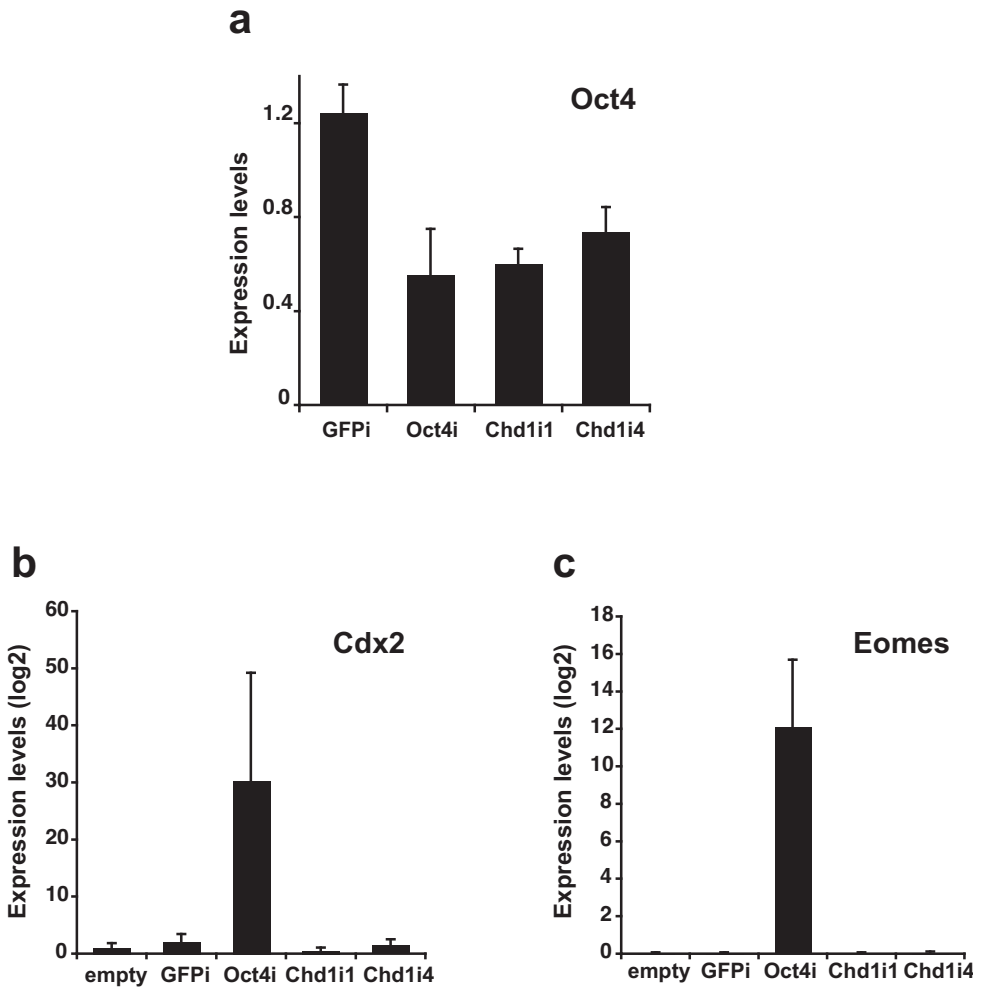

Supplementary Figure 3

Supplementary Figure 3. Knockdown of *Chd1* leads to a reduction in the level of *Oct4* but does not induce expression of trophectoderm markers. a, Expression levels of *Oct4* were analyzed by qRT-PCR in infected E14 cells (isolated by FACS for mCherry) on passage 2. *Chd1* RNAi, using either shRNA, lead to a reduction in the levels of *Oct4* mRNA to about half, similar to that observed in *Oct4* RNAi. The values are represented as mean ± s.d. (n=3). **b, c,** *Oct4* RNAi, but not *Chd1* RNAi, leads to expression of the trophectoderm markers *Cdx2* **(b)** and *Eomes* **(c)**, measured by qRT-PCR. The values are represented as mean ± s.d. (n=3).

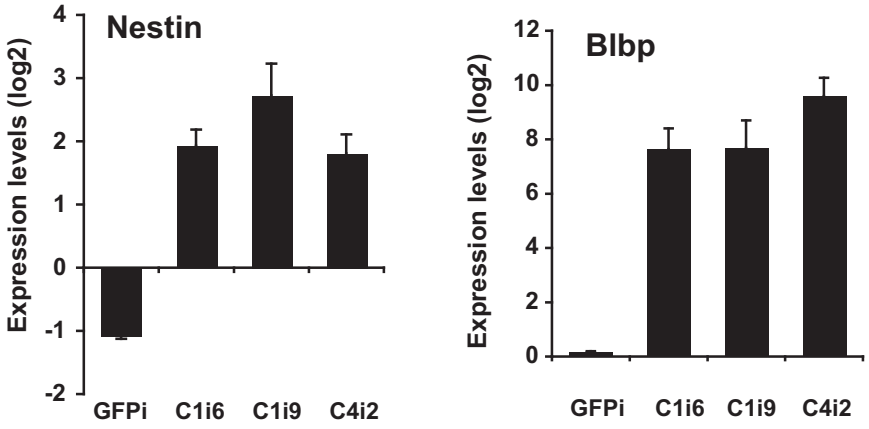

Supplementary Figure 4

Supplementary Figure 4. qRT-PCR validation of neural percursors expression in Chd1i cells . Up-regulation of neural markers in Chd1i cells, first detected with expression profiling using microarrays, was confirmed with qRT-PCR for *Nestin* and *Blbp*. The values are represented as mean ± s.d. (n=3).

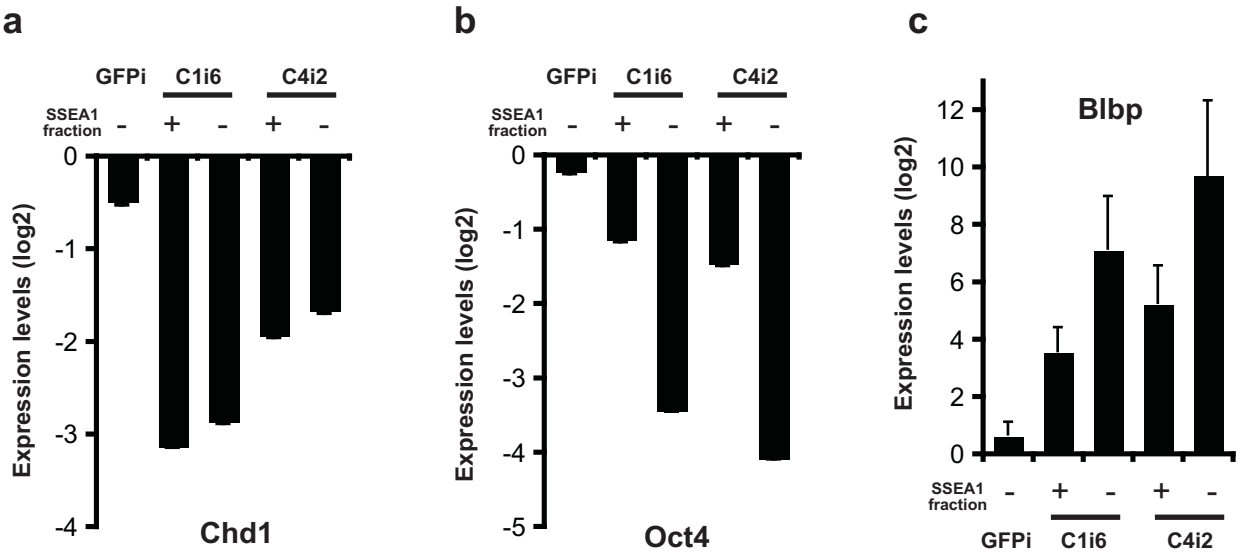

Supplementary Figure 5

Supplementary Figure 5. Analysis of Chd1i cells differentiation using the ES cell surface marker SSEA1. Live cells (PI negative) of Chd1i clones and control GFPi were sorted using the surface marker SSEA1. RNA from both SSEA1+ and SSEA1- fractions was collected and analyzed by qRT-PCR. **a,** Down-regulation of *Chd1* was confirmed in SSEA1+ and SSEA1- cells. **b,** SSEA1- Chd1i cells have consistently lower levels of *Oct4* when compared to SSEA1+ Chd1i cells. **c,** *Blbp* is already detected in Chd1i SSEA1+ cells and is highly induced in SSEA1- Chd1i cells, but not GFPi cells. The values are represented as mean ± s.d. (n=3), and are representative of 2 independent FACS experiments.

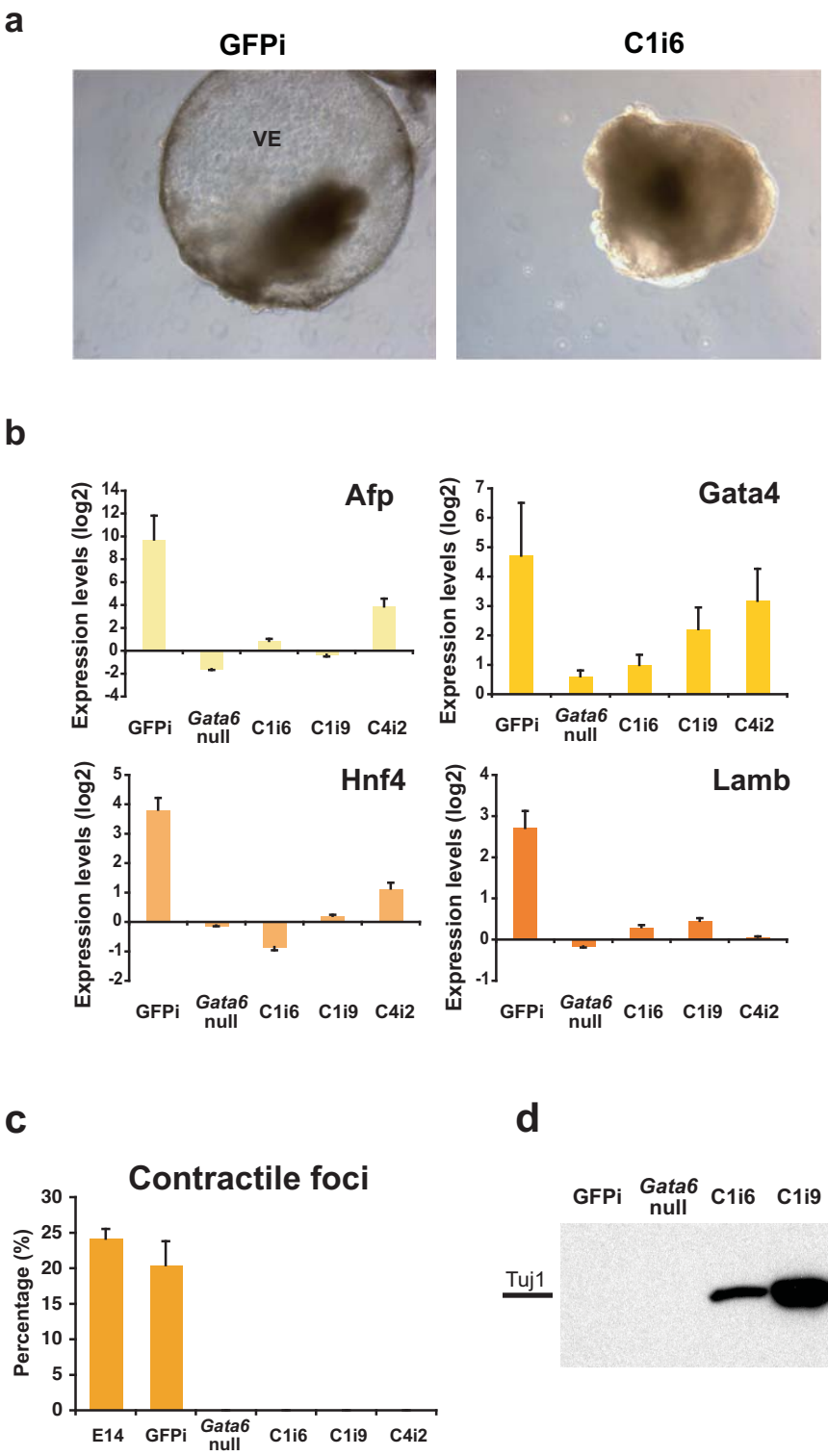

Supplementary Figure 6

Supplementary Figure 6. Chd1i cells have impaired differentiation. a, ES cells were cultured in non-attachment conditions and without LIF to form embryoid bodies (EBs). Chd1i EBs lack visceral endoderm cysts (V.E.), as seen in bright field images (10 day EBs). **b,** Expression of primitive endoderm markers was analyzed in EBs at day 6. All three Chd1i clones tested showed reduced expression of *Afp, Gata4, Hnf4* and *Lamb*, similar to *Gata6*-/- cells. The values are represented as mean ± s.d. (n=3). **c,** EBs plated for 12 days were analyzed for foci of contractile cardiac muscle. *Gata6*-/- cells and Chd1-deficient cells did not have any EBs with contractile foci. The values are represented as mean ± s.d. (n=3). **d,** Whole cell extracts of day 6 EBs were collected and equal amounts of total protein were loaded for western blot analysis. The neuronal marker Tuj1 is strongly detected in Chd1i EBs.

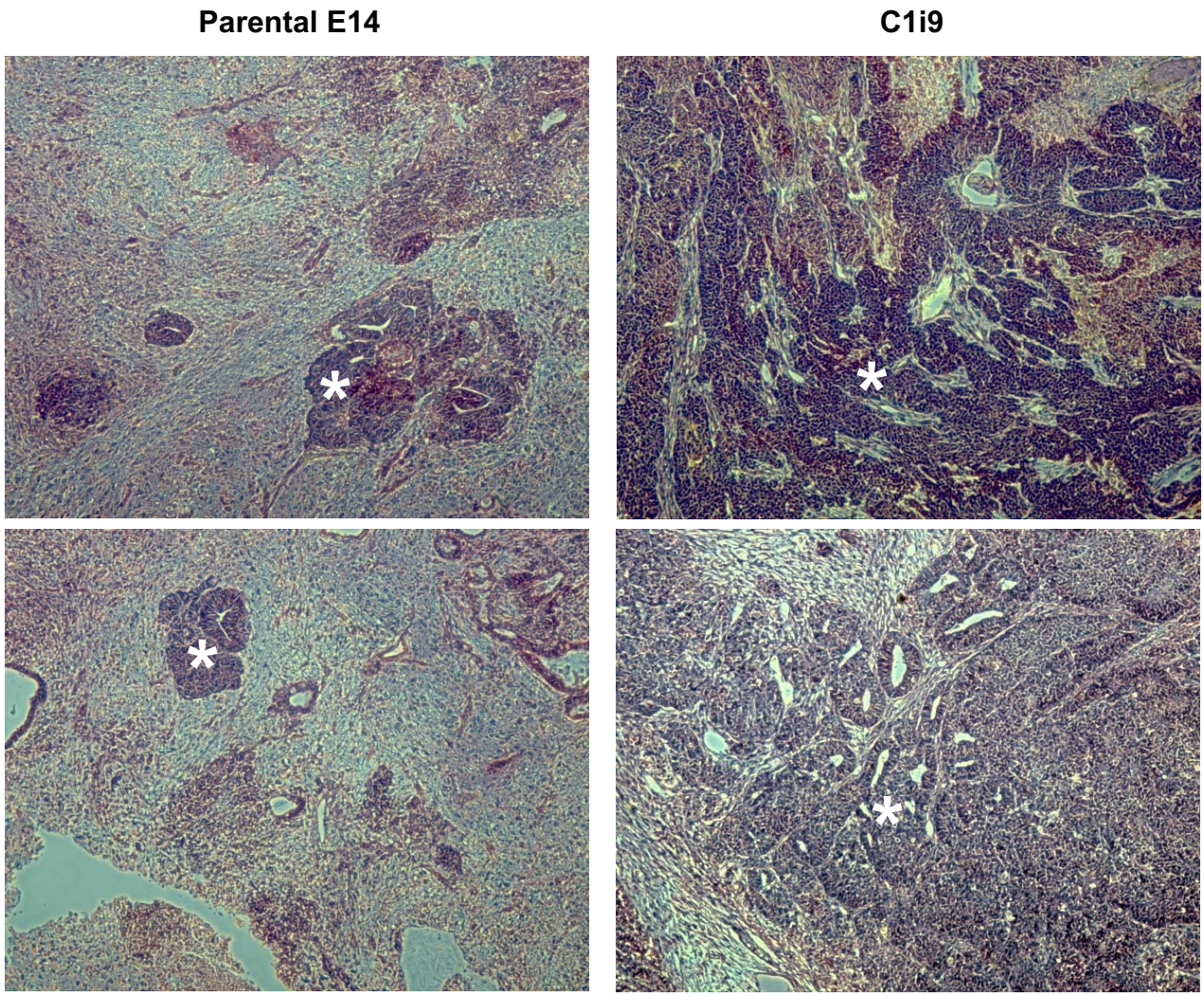

Supplementary Figure 7

Supplementary Figure 7. Teratomas from Chd1i ES cells have abundant neural differentiation. Parental E14 cells and Chd1i ES cells were introduced into immunocompromised SCID mice to form teratomas. Analysis of the teratomas after 12 weeks shows abundant neuroectoderm tissue (white asterisk) as compared to parental ES cells.

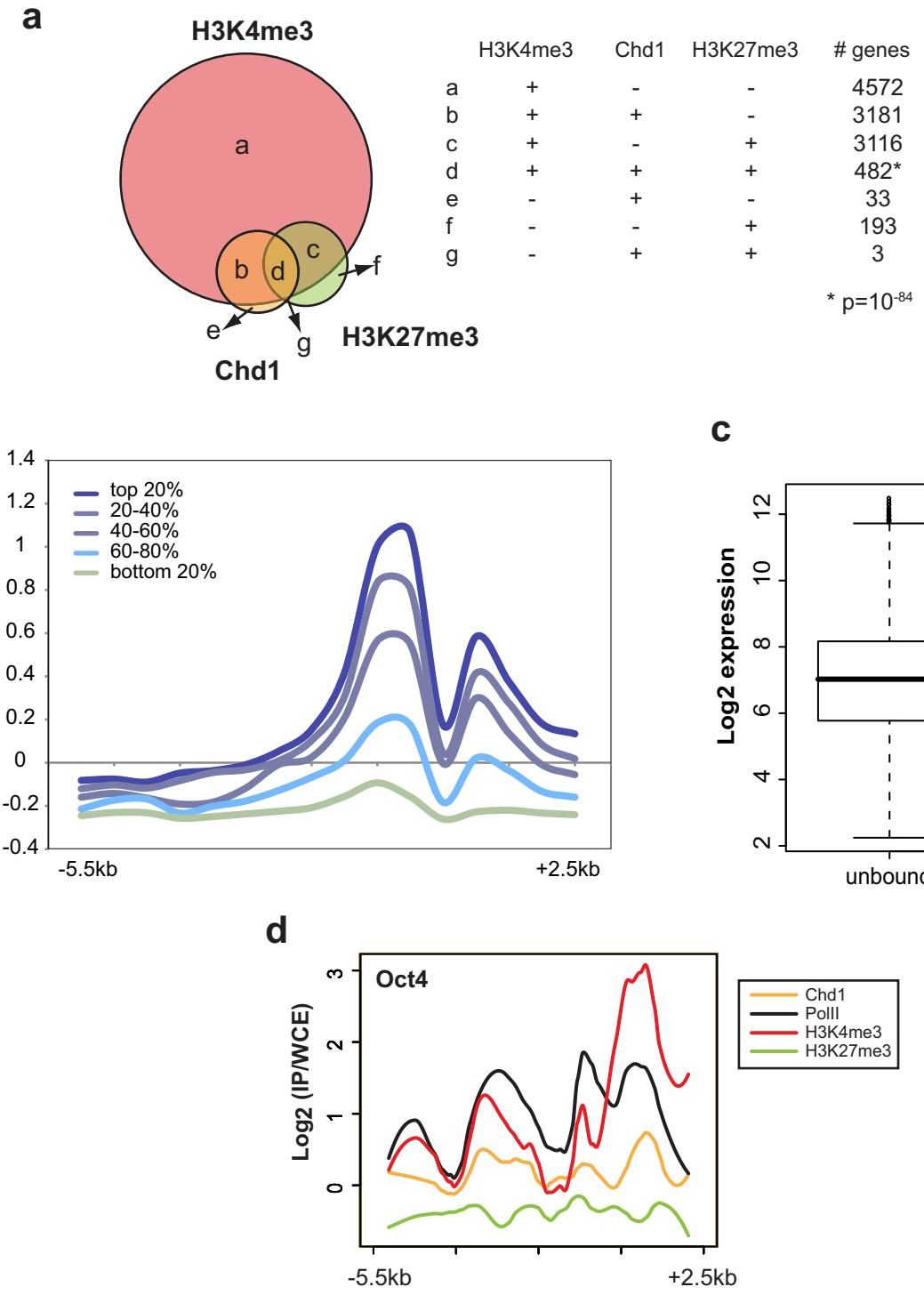

Supplementary Figure 8

Supplementary Figure 8. Genome-wide analysis of Chd1 binding in ES cells using chromatin immunoprecipitation and microarrays. a, Chd1 targets are trimethylated at histone H3 K4. Venn diagram demonstrating the overlap of Chd1, H3K4me3 and H3K27me3 target genes. Numbers of genes for each section of the Venn diagram are given in the table. Target genes were determined using the Young lab algorithm as described in the Materials and Methods section. Only 482 genes with bivalent domains (positive for both H3K4me3 and H3K27me3) are bound by Chd1. The data indicate that Chd1 is significantly under-represented in bivalent domains as determined by the hypergeometric test for the ratio of the probability of Chd1 targets found in bivalent genes to that found in non-bivalent genes. **b,** Chd1 bound targets are highly expressed. All genes were classified into 5 groups depending on their expression as indicated. Average log2(IP/input) ratios for 16 500bp windows along 8kb promoter region for each expression group were plotted. Note enrichment of Chd1 is highest in the 20% most highly expressed genes in ES cells. **c,** Genes that are bound by Chd1 in ES cells have a higher median of expression than those that are not bound. The p-value was calculated using the t-test. **d,** Chd1 is enriched immediately adjacent to transcription start site of *Oct4*. The *Oct4* gene is bound by Chd1 (following the Young lab algorithm). The graph plots log2(IP/input) ratios of probes for Chd1, H3K4me3, H3K27me3 and PolII binding or enrichment over the 8kb promoter region of the Oct4 gene.

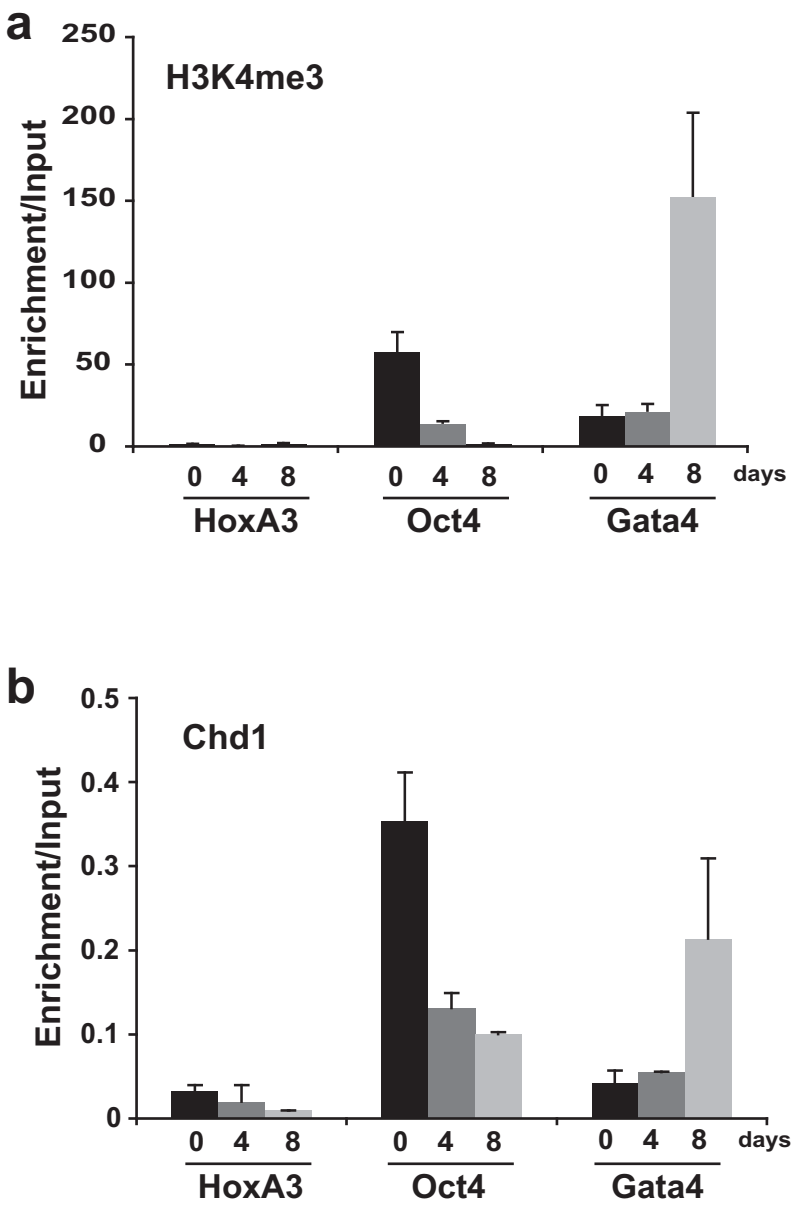

Supplementary Figure 9

Supplementary Figure 9. Chd1 binding coincides with H3K4me3 upon EB differentiation. a, b, During EB differentiation of mouse E14 ES cells (days 0, 4, 8) both H3K4me3 **(a)** and Chd1 **(b)** enrichment is lost in the promoter region of *Oct4* , and increases at the promoter of *Gata4*. The values are represented as mean ± s.d. (n=3). The promoter of HoxA3 is a control gene known to not be marked with H3K4me3 in ES cells (Bernstein *et al*. 2006).

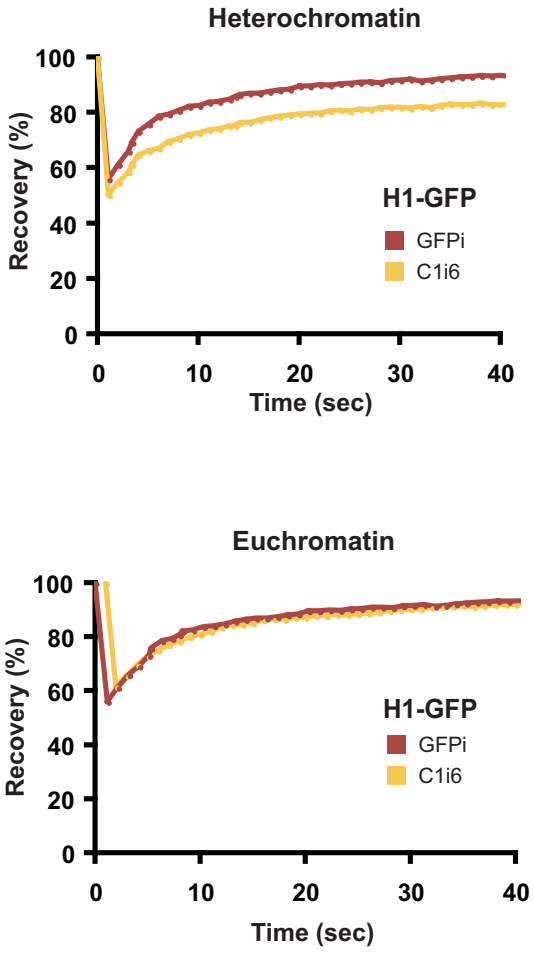

Supplementary Figure 10. FRAP analysis of H1-GFP in control GFPi and Chd1i ES-like cells. Chd1i ES-like cells have a significant delay in H1-GFP protein exchange in heterochromatin but not euchromatin. Values are representative of two independent experiments and the error bars are between 3 and 8%.

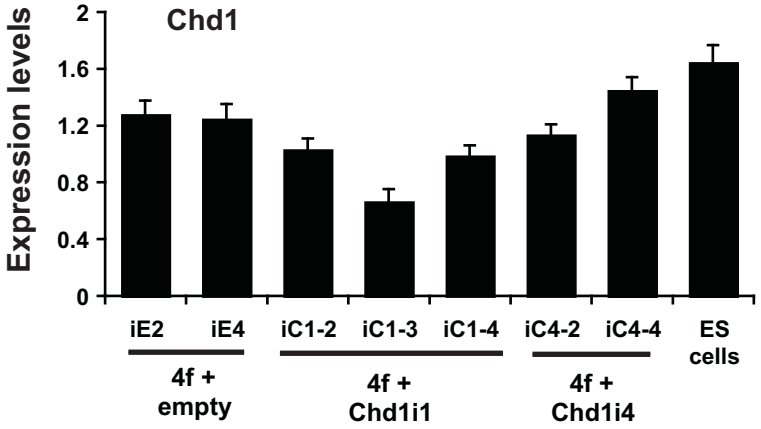

Supplementary Figure 11

Supplementary Figure 11. *Chd1* levels in reprogrammed iPS cells. Expression of *Chd1* was analyzed in colonies expanded from empty vector- or Chd1RNAi vector-infected cells (along with the four reprogramming factors). Data is shown relative to a 4F+Empty iPS clone (iE1). No signifcant differences between the control and the Chd1i iPS lines. The values are represented as mean ± s.d. (n=3).

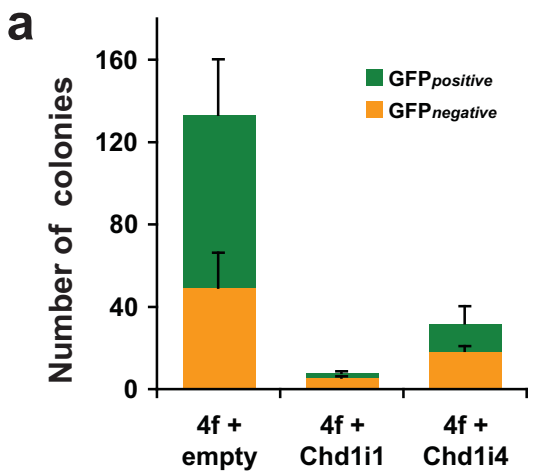

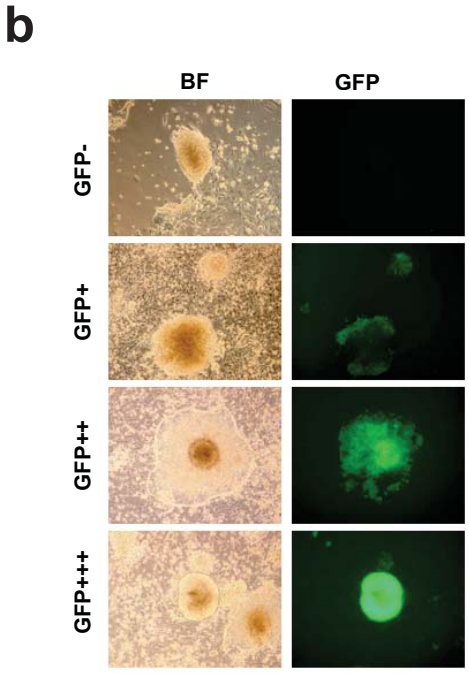

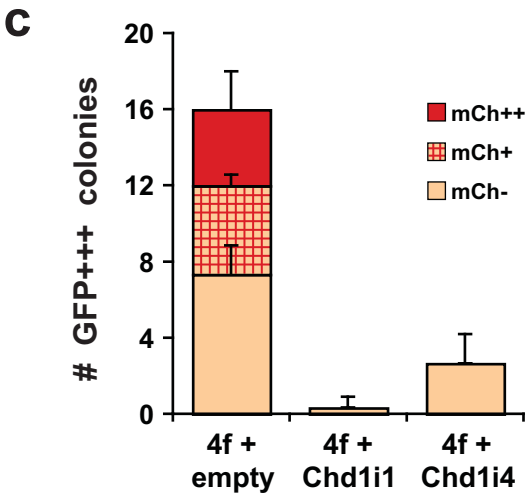

	4f + empty			4f + Chd1i1			4f + Chd1i1		
mCherry	-	+	++	-	+	++	-	+	++
well1	7	5	2	0	0	0	3	0	0
well2	9	4	6	1	0	0	4	0	0
well3	6	5	4	0	0	0	1	0	0
average	7.3	4.7	4.0	0.3	0.0	0.0	2.7	0.0	0.0
st.dev	1.5	0.6	2.0	0.6	0.0	0.0	1.5	0.0	0.0

Supplementary Figure 12

Supplementary Figure 12. Analysis of the expression of the lentiviral vector for RNAi upon reprogramming using the reporter gene mCherry. This assay was performed with a higher infection efficiency (Wernig et al. Nat Biotech, 26(8): 916-24, 2008), in which the RNAi virus is added at lower cell density (40,000 cells per 6well) and at the same time as the four reprogramming factors. **a,** The number of colonies was scored both by morphology and GFP expression. The values are represented as mean ± s.d. (n=3). **b,** Oct4-GFP colonies were scored using 4 categories (GFP-, GFP+, GFP++, GFP+++) depending on the number of GFP positive cells. **c,** Only GFP+++ colonies were scored according to their mCherry expression. These represent colonies that are considered fully reprogrammed. No GFP+++/mCherry+ colonies were found when Chd1 RNAi vector was added. The values are represented as mean ± s.d. (n=3). Number of colonies are shown in the table below.

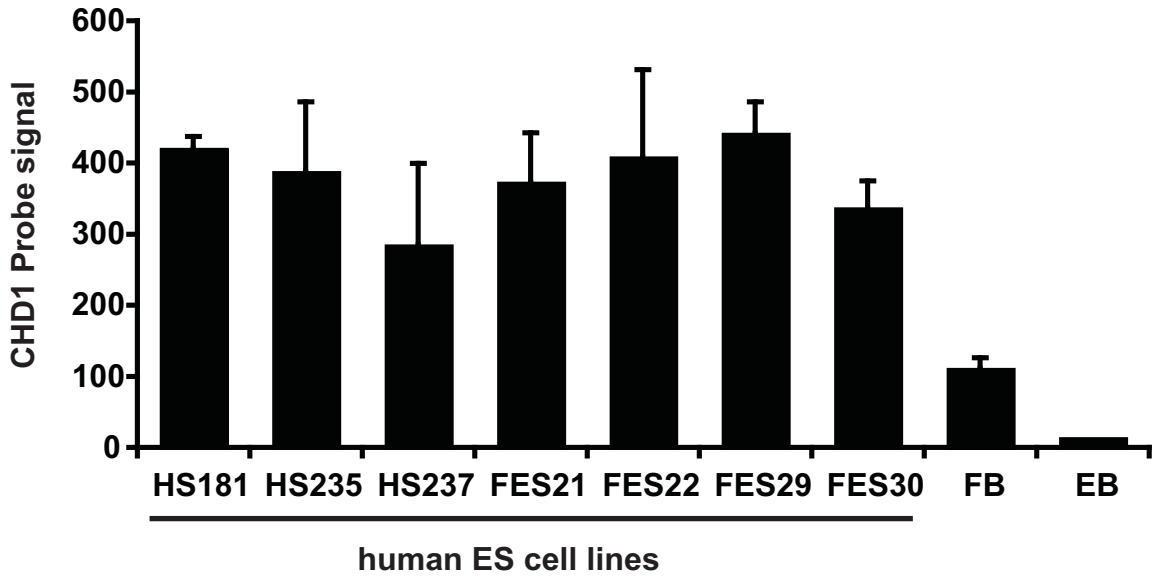

Supplementary Figure 13

Supplementary Figure 13. Microarray analysis of *CHD1* expression in several human ES cell lines. Transcriptional profile of seven different independently-derived human ES cell lines show up-regulation of *CHD1* when compared to foreskin fibroblasts (FB) and EB-derived differentiated cells (EB) . Data analyzed from Skottman *et al.* 2005 (*Stem cells*, 23(9): 1343-56).